




Review

Magnetic Resonance Spectroscopy in Diagnosis and Follow-Up of Gliomas: State-of-the-Art

Malik Galijasevic ^{1,2,†} , Ruth Steiger ^{1,2,†} , Stephanie Mangesius ^{1,2,*} , Julian Mangesius ³ , Johannes Kerschbaumer ⁴ , Christian Franz Freyschlag ⁴ , Nadja Gruber ^{5,6} , Tanja Janjic ^{1,2} , Elke Ruth Gizewski ^{1,2}  and Astrid Ellen Grams ^{1,2} 

¹ Department of Neuroradiology, Medical University of Innsbruck, 6020 Innsbruck, Austria; malik.galijasevic@i-med.ac.at (M.G.); ruth.steiger@i-med.ac.at (R.S.); tanja.janjic@i-med.ac.at (T.J.); elke.gizewski@i-med.ac.at (E.R.G.); astrid.grams@i-med.ac.at (A.E.G.)

² Neuroimaging Research Core Facility, Medical University of Innsbruck, 6020 Innsbruck, Austria

³ Department of Radiation Oncology, Medical University of Innsbruck, 6020 Innsbruck, Austria; julian.mangesius@i-med.ac.at

⁴ Department of Neurosurgery, Medical University of Innsbruck, 6020 Innsbruck, Austria; j.kerschbaumer@i-med.ac.at (J.K.); christian.freyschlag@i-med.ac.at (C.F.F.)

⁵ VAScAge-Research Centre on Vascular Ageing and Stroke, 6020 Innsbruck, Austria; nadja.gruber@uibk.ac.at

⁶ Department of Applied Mathematics, University of Innsbruck, 6020 Innsbruck, Austria

* Correspondence: stephanie.mangesius@i-med.ac.at

† These authors contributed equally to this work.

Simple Summary: Magnetic resonance spectroscopy (MRS) is a useful technique in diagnosis and follow-up of gliomas. In this review we provide an insight in the use of both proton and phosphorous MRS in clinical and scientific every day practice.

Abstract: Preoperative grade prediction is important in diagnostics of glioma. Even more important can be follow-up after chemotherapy and radiotherapy of high grade gliomas. In this review we provide an overview of MR-spectroscopy (MRS), technical aspects, and different clinical scenarios in the diagnostics and follow-up of gliomas in pediatric and adult populations. Furthermore, we provide a recap of the current research utility and possible future strategies regarding proton- and phosphorous-MRS in glioma research.

Keywords: magnetic resonance spectroscopy; glioma; imaging biomarkers



Citation: Galijasevic, M.; Steiger, R.; Mangesius, S.; Mangesius, J.; Kerschbaumer, J.; Freyschlag, C.F.; Gruber, N.; Janjic, T.; Gizewski, E.R.; Grams, A.E. Magnetic Resonance Spectroscopy in Diagnosis and Follow-Up of Gliomas: State-of-the-Art. *Cancers* **2022**, *14*, 3197. <https://doi.org/10.3390/cancers14133197>

Academic Editor: Carmen Balana

Received: 15 May 2022

Accepted: 27 June 2022

Published: 29 June 2022

Publisher's Note: MDPI stays neutral with regard to jurisdictional claims in published maps and institutional affiliations.



Copyright: © 2022 by the authors. Licensee MDPI, Basel, Switzerland. This article is an open access article distributed under the terms and conditions of the Creative Commons Attribution (CC BY) license (<https://creativecommons.org/licenses/by/4.0/>).

1. Introduction

Correct and timely diagnosis of a glioma is extremely important. Patients benefit from an early diagnosis and precise follow up. Early diagnosis can have an impact on quality of life and overall prognosis [1,2], and the importance of correct follow-up is well known in all tumor types and subtypes. With an increase in our knowledge of glioma pathology, conventional MRI is struggling in our experience especially in follow-up and distinguishing radiation necrosis (RN), pseudoprogression (PsP), and tumor progression (TP) in high grade gliomas. Besides regular structural sequences, in the diagnosis and follow-up of these tumors, additional sequences are used to provide further information about the pathological processes in gliomas [3], or the standard sequences are being quantified in order to differentiate between different pathological tumor types [4]. To this end, in our centre we routinely use perfusion weighted imaging (PWI), delayed contrast-enhanced imaging, and proton-MRS.

MRS is a special magnetic resonance technique used to quantify different metabolites in a voxel (volume pixel) of tissue. So far in clinical practice only hydrogen (¹H), or proton-MRS is used, although an MRS spectrum can be obtained from any element with non-zero spin. MRS with other chemical elements has been used in research purposes

(most commonly phosphorous— ^{31}P and carbon— ^{13}C). The main metabolites in ^1H -MRS in clinical settings are N-acetylaspartate (NAA), choline (Cho), and creatine (Cr). It is a well known technique used in clinical practice in the diagnosis and follow up of various brain lesions [5,6]. The main metabolites in ^{31}P -MRS are phosphocreatine (PCr), adenosine triphosphate (ATP), inorganic phosphate (Pi), phosphomonoesters (PME) and phosphodiesters (PDE). In addition, intracellular pH and magnesium levels can be calculated.

As an example of tumor protocol MRI, patients with brain tumors can be imaged using sequences described in the consensus recommendations by Ellingson et al. [7]. If the needed hardware and software allow, these basic sequences can be supplemented with some of the more advanced techniques in order to better discriminate between various subtypes of tumors, as described by Malik et al. [8]. In our center the patients with brain tumors are imaged with 3 T and 1.5 T machines with the following sequences: axial T2-turbo spin echo (TSE), 3D fluid-attenuated inversion recovery (FLAIR), axial diffusion weighted imaging (DWI), axial susceptibility-weighted imaging (SWI) and 3D T1 magnetization prepared—rapid gradient echo (MPRAGE) before and after contrast application. Besides these “classical” sequences, we use PWI, MRS, and delayed post-contrast imaging in order to predict pathological diagnosis, monitor answer to therapy, radiation changes, and possible recurrence of a disease. If the tumor is localised in proximity to the eloquent cortical centers, we use functional magnetic resonance imaging (fMRI) with motor and language paradigms to access possible infiltration and to plan surgical approach (only on 3 T scanners).

In light of a recent publication by the World Health Organization (WHO) Classification of Tumors of Central Nervous System in 2021, in addition to significant changes in the classification of gliomas, it is important to provide an update regarding the place of MRS in the diagnostics, follow up, and research of gliomas. Since it is based on molecular features, the WHO Classification of Tumors of Central Nervous System (2021) introduced many changes for glial brain tumors. Thus, it is of outmost importance to review the value of commonly available ^1H -MRS and the novel ^{31}P -MRS in both classifying the tumor subtype before resection and distinguishing RN, PsP and TP during follow-up. There is already a great number of reviews and original research papers dealing with MRS in gliomas, however, to the best of our knowledge this is the first review analysing this topic regarding the new WHO classification. The aim of this review is to provide an overview of the clinical state-of-the-art of this rapidly evolving technology in the diagnostic work up of glioma patients by means of MRS, and to further contribute to the planning of future research studies by enabling better preoperative and postoperative radiological assessment of gliomas in light of the new WHO-classification. While MRS in the adult population has been extensively explored in the literature, little has been described about its value in the pediatric population. For this reason, a comparison of MRS examination and interpretation between adult and pediatric patients in the context of neuro-oncology assessment is presented here.

2. Classification of Gliomas

In 2016 the WHO for the first time included molecular parameters in the final diagnosis of tumors of the central nervous system [9]. This was underlined in a new version of the classification in 2021, in which some of these molecular markers were made even more important than the histological appearance. Furthermore, some new tumor types and subtypes were introduced [10].

Besides purely didactic changes like using Arabic instead of Roman numerals in the designation of grade, or using “type” and “subtype” instead of “entity” and “variant”, the new classification also brought some more clinically important changes. As previously mentioned, in some cases the molecular features supersede histologic characteristics. For example, histologically “low-grade” astrocytoma, IDH-wildtype (IDH-wt) and EGFR-amplification, TERT-promotor mutation, or combined gain of chromosome 7 and loss of chromosome 10, can be considered as glioblastoma (GBM), and consequently as WHO

Grade 4 [10]. The new classification of gliomas with the most important molecular features is given in Table 1. Some of the tumor types are newly recognised, and have not yet been given a WHO grade.

Table 1. Classification of gliomas according to the new 2021 WHO Classification [10]. The abbreviations are given in the Abbreviations section.

	WHO Grade	Most Common Molecular Features
Circumscribed gliomas		
Pilocytic astrocytoma	1	KIAA1549-BRAF [11]
High-grade astrocytoma with piloid features	new subtype	specific DNA-methylation profile [12]
Pleomorphic xanthoastrocytoma	2, 3	BRAF [13]
Subependymal giantcell astrocytoma	1	TSC1, TSC2 [14]
Chordoid glioma	2	PRKCA [15]
Astroblastoma, MN1-altered	new subtype	MN1 [16]
Pediatric diffuse low grade gliomas		
Diffuse astrocytoma, MYB- or MYBL1-altered	1	MYB, MYBL1 [17]
Angiocentric glioma	1	MYB [10]
Polymorphous low-grade neuroepithelial tumor of the young	1	PLNTYs, BRAF, FGFR [18]
Diffuse low-grade glioma, MAPK pathway-altered	new subtype	FGFR1, BRAF [19]
Pediatric-type diffuse high-grade gliomas		
Diffuse midline glioma, H3 K27-altered	4	H3 K27 [20]
Diffuse hemispheric glioma, H3 G34-mutant	4	H3F3A (G34R/V) [21], GFAP [22], p53 [23]
Diffuse pediatric-type high-grade glioma, H3- and IDH-wt	4	IDH-wt, H3-wt, MYCN, PDGFRA [24]
Infant-type hemispheric glioma	new subtype	NTRK, ALK, ROS1, MET [25]
Adult-type diffuse gliomas		
Astrocytoma, IDH-mutant	2, 3, 4	IDH1, IDH2 [26], ATRX [27]
Oligodendroglioma, IDH-mutant, and 1p/19q-codeleted	2, 3	IDH [28], 1p19q-codeletion, ATRX, p53 [29]
Glioblastoma, IDH-wt	4	no IDH mutation (IDH-wt), ATRX, TERT [30]

3. Technical Overview

3.1. Pediatric Population

Newborns until up to 3–4 months can be examined by the feed and wrap technique using special ear cuffs and a vacuum pillow without sedation but with constant monitoring of oxygen saturation by a neonatologist. For older babies and young children, until about reaching the school age, MRI examinations usually have to be acquired under general anesthetic, certainly including the monitoring of vital functions.

3.2. Older Children and Adults

For older children and adults (under the condition of compliance and physical feasibility) the MR spectroscopy measurement procedure is identical to structural imaging of the brain. Ear protection for noise reduction is mandatory for all age cohorts and all MRI field strengths. In the next two subsections an example of standardized spectroscopy sequence planning is given.

3.3. Sequence Planning—1H-MRS

Planning of the spectroscopy sequence (chemical shift imaging—CSI vs. single voxel spectroscopy—SVS) particularly depends on the location of the brain region under investi-

gation and the medical purposes. Shimming for routine patients is performed automatically, whereas, for study participants and scientific investigations, it is carried out manually in order to avoid line broadening of the spectral width at the half amplitude of the signal (FWHM) at physical values for 1.5 T: SVS < 13 Hz, CSI < 15 Hz and at 3 T: SVS < 20 Hz, CSI < 25 Hz [31].

3.4. Sequence Planning—³¹P-MRS

³¹P-MRS is performed in a 3 T MRI machine using a double-tuned ¹H/³¹P volume head coil (Rapid Biomedical, Würzburg, Germany). The sequence is planned on an isotropic T2-weighted 3D sequence. Boundary regions, as well as regions filled with air or bone are spared, to avoid voxel contamination. The measurements are acquired using the parameters given in Table 2, and based on a conventional sequence by Siemens and described by Hattingen et al., in order to ensure reproducibility and applicability for potential future clinical use [32–34].

Table 2. Used parameters for ³¹P-MRS acquisition.

Matrix	8 × 8 × 8
Field of view	240 × 240 × 200 mm ³
Voxel size	30 × 30 mm ²
Slice thickness	25 mm
Repetition time	2000 ms
Echo time	2.3 ms
Flip angle	90°

4. Diagnosis and ¹H-MRS

4.1. Pediatric Population

The most common glioma in the pediatric population is pilocytic astrocytoma [35]. This tumor type is not only the most common glioma, but is the most common brain tumor in children in general, accounting for around 15% of all brain tumors in this population [36]. The imaging of the pilocytic astrocytoma is fairly straightforward using regular structural MRI sequences, however, when performed, MRS show a high Cho/NAA and Cho/Cr ratio, and low Cr with a decreased NAA/Cr ratio [37]. These changes can be seen in an example of a 2 year old patient with histologically proven cerebellar pilocytic astrocytoma (Figure 1).

High-grade gliomas, not otherwise specified (NOS) are the most common high-grade gliomas in children [35]. There is not much difference in interpreting spectroscopy findings in children compared to those of adults. The best indicator of malignancy was found to be the NAA/Cho ratio. High-grade astrocytic tumors tend to have more decreased NAA and increased Cho compared to the lower-grade tumors [38]. However, as can be appreciated in our real-world example, relying solely on a spectroscopy can be misleading, especially in differentiating various diffuse tumors (as in our example in Figure 2), as both, lower and higher grade diffuse tumors can have similar spectra, albeit a difference between diffuse and circumscribed gliomas is usually clear (Figure 1 vs. Figure 2).

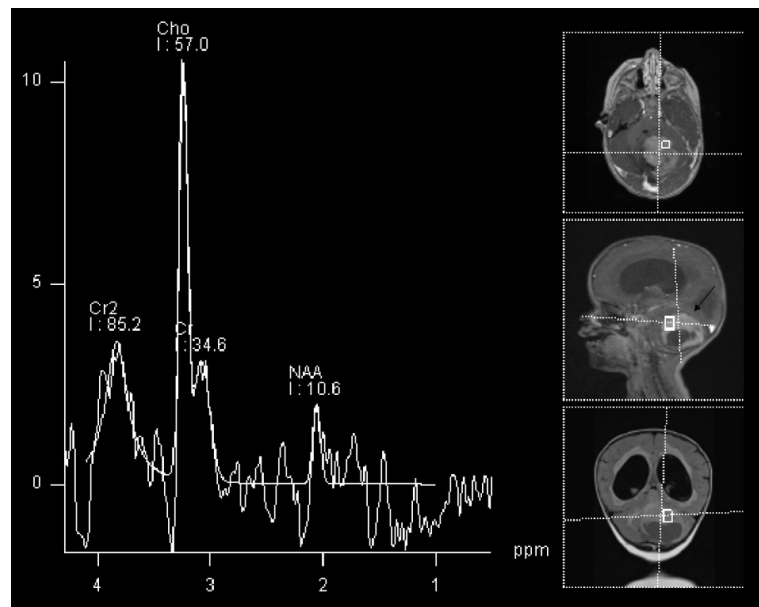


Figure 1. 1H-MRS in a patient (2 Y) with pilocytic astrocytoma (black arrow). Significantly increased Cho and decreased NAA and Cr are observed.

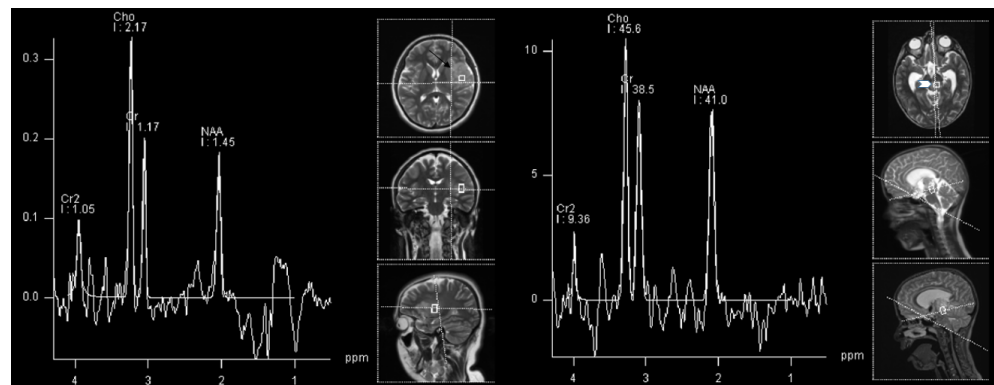


Figure 2. 1H-MRS in a patient (15 Y) with astrocytoma grade 3 (left, black arrow) and in a patient (8 Y) with astrocytoma WHO grade 2 (right, white arrowhead). Similar spectra are present in both grade 3 and grade 2 astrocytoma with increased Cho and decreased NAA, with the absence of Cr decrease.

4.2. Adult Population

4.2.1. Low-Grade vs. High-Grade

Preoperative grading of gliomas can be difficult based on conventional MRI, especially with the absence of significant edema and/or contrast-enhancement. This is a common diagnostic challenge, even in high-grade tumors. In the case of diagnostic uncertainty, additional information can be obtained with MRS [39,40].

In gliomas, the general rule is that the NAA and Cr decrease, and other metabolites increase with higher tumor grades. Some authors suggest using a Cho/NAA ratio greater than 2.2 to predict higher grade, and a presence of myo-inositol to predict the lower grade lesions [41,42]. However, as shown in Figure 3 and in our own experience, low-grade gliomas can also have similar spectra as high-grades (but rarely vice-versa).

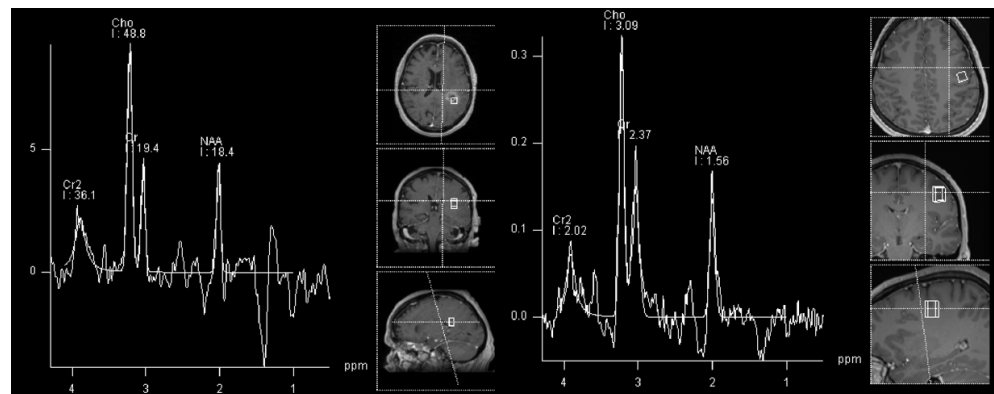


Figure 3. Similar ^1H -MRS spectra can be appreciated in an adult patient with glioblastoma (left, black arrow) and in a patient with astrocytoma WHO grade 2 (right, white arrowhead) with increased NAA and decreased Cr and Cho.

4.2.2. Follow-Up and MRS

MRS is important in postoperative follow up, especially in high grade gliomas. As previously described, MRS is used as a valuable tool in the diagnosis and follow-up of gliomas [43]. Both residual tumor or tumor recurrence may be observed after brain irradiation. Furthermore, PsP and RN constitute two further different types of adverse therapeutic effects.

Radionecrosis is determined as the development of necrotic brain tissue after irradiation, which emerges between three months and one year after radiotherapy [22] and affects about 20% of radiotherapy in GBM patients [44] especially after receiving higher radiation doses [45] and additional chemotherapy [46].

PsP is defined as a transient and self-limited volume increase without evidence of vital tumor, which occurs between two and five months after the initiation of radiation, and affects approximately 20% of patients with concomitant chemo-radiation. It is assumed to be a mixed effect of treatment reaction and a collapse of the blood-brain barrier [44]. As differentiation from recurrent tumor is difficult, a close monitoring with frequent MRI is recommended so as not to misinterpret an RN and PsP [47].

Due to the expected high rate of treatment effects, and the fact that each of the three above-mentioned post therapeutic conditions require different therapeutic strategies [44], monitoring is crucial.

Failing to differentiate radiation induced changes or drug-induced PsP from TP can have dire clinical consequences.

The effect of radiotherapy on the brain are early alterations in metabolic activity, which finally result in tissue degradation, yet antecede the development of symptoms and occur before evidence of changes can be determined on structural images using conventional MRI in early post treatment scans [48].

The differentiation between PsP and TP with MRS poses a major diagnostic challenge, particularly with the use of single-voxel acquisitions, as discussed herein. Both types of lesions can demonstrate neuronal loss/dysfunction (decrease of NAA), abnormal cellular membrane attenuation/integrity and proliferation (increase of Cho), and anaerobic metabolism (high Lac/lipid ratio). An increased Cho/NAA and Cho/Cr ratio corresponds with tumor recurrence [49–54]. PsP could be diagnosed based on elevated lipid signals on MRS [55]. However, these effects may not always be seen, as the absence of Cho or a low Cho/NAA ratio has also been observed. Contrarily, patients with TP present with lower lipid signals and a high Cho/NAA ratio. The evidence of elevated lipid signals, together with a low Cho/NAA ratio, may help to distinguish PsP from TP [52].

Consequently, the most important metabolite in differentiating TP from radiation-induced PsP is choline, as disturbances in the biosynthesis of cell membranes and metabolic turnover are reflected by an increase in choline. As in a primary tumor, choline will be

increased in TP, whereas it will be decreased in RN and radiation induced PsP, together with NAA and creatine. In our experience, the most common clinical encounter is with patients that have imaging characteristics of both TP and radiation-induced PsP (Figure 4).

In radionecrosis, progressive metabolic changes induce a decreased concentration of the neuronal marker N acetylaspartate (NAA), which reflects cell death by apoptosis or neuronal dysfunction. Disturbed biosynthesis of cell membranes and metabolic turnover are reflected by an increase in choline (Cho). However, creatinine (Cr), which constitutes the marker of energy metabolism, is considered to be unaffected by radiation damage. Therefore, in brain tissue developing radionecrosis increased Cho/Cr ratio is observed [6,53,54,56–58].

A meta-analysis involving 1174 patients treated for GBM could show that using advanced MRI techniques leads to greater diagnostic accuracy when compared to using only conventional MRI for follow-up of response to treatment, leading to greater sensitivity and specificity [59]. It has recently been suggested [60] that for the differentiation of PsP, RN and TP, DWI and PWI should be performed after conventional sequences. However, in the case of remaining diagnostic uncertainty, MRS was shown to provide complementary information. Some studies described cut-off values for differential diagnosis.

For differentiating between PsP and TP, the following MRS ratios and cut-offs were suggested: a Cho/NAA ratio under 1.47–2.11 and Cho/Cr ratio under 0.82–2.25 indicated PsP. Cho/NAA ratio had a mean of 2.72 for TP, and 1.46 for RN ($p < 0.01$) [61]. Figure 4 shows the Cho/NAA ratio under cut-off for histologically confirmed GBM progression.

Ultimately, several advanced MRI modalities, including MRS, seem to improve differentiation between PsP, RN and TP, compared with conventional MRI.

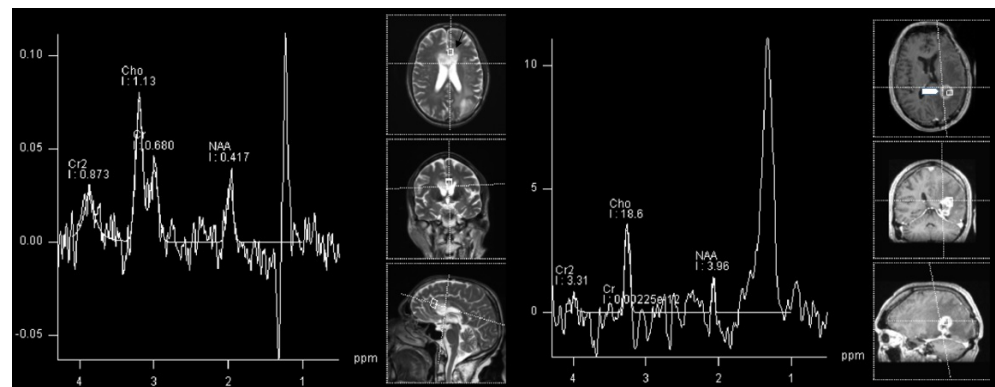


Figure 4. 1H-MRS in an adult patient with glioblastoma progression (**left**, black arrow) and in a patient with signs of both progression and radiation necrosis (**right**, white arrowhead). Cho/NAA ratio is under proposed cut-off for TP in progressive GBM.

5. Future Aspects and 31P-MRS

1H-MRS is a well established technique in clinical practice for the diagnosis and follow-up of glioma. As previously discussed, depicting the various 1H-metabolites can bring the necessary information for classifying a brain lesion, and especially to monitor the answer to therapy and possible recurrence. Recently however, many research groups are trying to find a similar clinical place for 31P-MRS. It showed potential to further classify the tumors, and even predicting recurrence.

Future research strategies should focus on differences in MRS in tumors with various molecular footprints. In a recently published study, differences in energy metabolites of GBMs with variations in MGMT and EGFR status were shown. These results showed indications of faster cell reproduction in MGMT-methylated and EGFR-amplified tumors and higher apoptotic activity in EGFR-amplified tumors regardless of the MGMT-status [62]. Another study showed lower lactate levels and intracellular pH in IDH-mutant gliomas compared to IDH-wild type gliomas [63]. However, other 31P-MRS markers were not significantly altered and could not predict the IDH-mutation status [64]. The same group

also showed the ability of 31P-MRS to predict the site of progression of GBM under angiogenic therapy. Namely, the elevated intracellular pH was regarded as a predictor for a progression of recurrent GBM treated with bevacizumab [65].

It would be interesting to further examine the possibilities of both 1H and 31P MRS in preoperative assessment of different molecular markers and the possibility of this method to predict progression. Regarding the 2021 WHO Classification of CNS Tumors these methods could be helpful in distinguishing various subtypes of gliomas.

As already discussed, spectroscopy can also be a reasonable tool in distinguishing various changes in tumor metabolism after standard therapy regimen with chemotherapy and radiation. In a recent paper, differences in energy metabolism between tumors in various stages according to RANO criteria were used using 31P-MRS. Among other results, in progressive disease patients, normalisation of energy metabolites after the induction of therapy was seen [66]. In another study, among other results, regional differences between normal appearing brain and various tumor areas in patients with GBM were shown, also using 31P MRS. Contrast-enhancing areas had increased intracellular pH and magnesium levels, decreasing with the distance from the tumor. PCr/ATP, PCr/Pi, Pi/ATP, PDE/ATP, PDE/PCr, and PDE/Pi were lower in tumor voxels compared to the healthy-looking brain voxels, while PME/PDE, PME/ATP, and PME/PCr were increased in tumor voxels [67]. Similar results were found by Hmilicova et al. [68]. Lower PCR/Pi, PDE/ATP, and higher pH were also found in a study by Maintz et al. [69], while Bulakbasi et al. found similar results regarding the intracellular pH, Mg levels, and PCr/ATP, PCr/Pi, PME/ATP, and PDE/ATP ratios [70]. Hattingen et al. found decreased PCr/Pi and increased Pi/ATP in tumor areas in patients with recurrent GBM treated with bevacicunab [71]. This implied antitumoral effects of bevacicunab and impaired oxidative energy metabolism in GBM treated with this drug. Similar to the findings of Walchhofer et al., the group around Ha et al. found increased PME/PDE and PME/PCr ratios in tumor areas [72]. Kamble et al. also found similar results regarding to the PCr/ATP, PCR/Pi, and PME/PDE ratios [73].

6. Limitations

6.1. 1H-MRS

1H-MRS is a promising method, but encounters several limitations, e.g., lesions near the bone due to magnetic susceptibility artifacts [58]. In addition, spectroscopy can accurately distinguish tissues containing pure RN from pure recurrence. However, metabolite values are averaged within the studied voxel in monovoxel studies, and consequently the co-existence of both effects constitute a major challenge in the interpretation of resulting spectra [57]. In contrast, multivoxel spectroscopy enables a more thorough examination of metabolic changes.

A further consideration in 1H-MRS is voxel positioning: tumor recurrence may further be more accurately depicted by means of spectroscopy in areas which do not enhance, as well as in the adjacent white matter, as typical tumor spectrum profiles are often depicted in these areas [6]. A promising upcoming method is 3D echoplanar spectroscopic imaging, where a large volume can be analyzed with greater resolution [74].

Some pros and cons of using 1H-MRS in clinical practice is given in Table 3.

Table 3. Pros and cons of including 1H-MRS in a clinical routine of glioma imaging.

Pros	Cons
Important information about the nature of the lesions	Hardware, software and know-how considerations-cost
More accurate follow-up	Relatively time costly and artifact-prone sequence

6.2. 31P-MRS

The future clinical benefit of 31P-MRS still has to be verified with clinical and confirmatory studies. The clinical application of this method has remained limited until today due to several factors.

First of all, the restricted availability of the coils and the technique renders clinical establishment difficult, especially in non-specialized centers.

Due to varying MRI technique and field strength used in the published studies reliable comparison of data is challenging. Regardless of these limitations, standardization is also lacking due to the limited number of studies or case series available for direct comparison and confirmation of published findings. The small sample size of published studies plus the heterogeneity of tumor patients render it difficult to draw generally accepted conclusions for clinical application. Thus, confirmatory studies involving this imaging technique are needed to render the interpretation of 31p-MRS results into a clinical applicable routine procedure [32].

Furthermore, the effect of “voxel bleeding” due to a poor point spread function is an omnipresent problem in MRS. This effect can be minimized by choosing voxels in which the tissue to investigate is present in at least two-thirds of the voxel. This approach has been shown to be of high value to retrieve significant and reliable results [66].

Another important reason for the lack of clinical application has been the lack of mean normal values in healthy controls as a comparison for the use of 31P-MRS. Particularly the knowledge of differences in the brain depending on sex, age and brain region are crucial for the interpretation of derived results. In a large study, it was found that ATP-resynthesis, ATP-hydrolysis and energy demand vary between brain regions, age and sex. Therefore, these parameters also have to be taken into account when investigating cerebral energy metabolism under pathological conditions. This renders the interpretation of 31P-MRS even more challenging [33].

31P-MRS studies in neurooncology also have several limitations inherent to the aggressive nature of the investigated tumors and the rapidly deteriorating health condition of effected patients. As 31P-MRS scans are time-intensive and, this examination can be intolerable for some GBM patients, especially in later disease stages. Consequently, published 31P-MRS studies usually include a small number of patients for whom scans were available, as follow up examinations experience a large number of dropouts. Consequently, large cohort studies are sparse and consequently confirmatory studies for more recent findings still lacking. Although state-of-the-art therapy, GBM bears a short survival time, thus rendering this limitation difficult to overcome [66].

A particular challenge in tumor imaging are the poor signal-to-noise ratios and, therefore, a noisier baseline of the spectra in tumor regions, which might potentially lead to an exclusion of two metabolites from analyses [67].

Additionally, the energy and membrane metabolism is modified in the entire brain of patients with GBM, even in “normal-appearing” brain areas and the contralateral hemisphere. Although GBM is an aggressive infiltratory process, this might also be explained by therapeutic effects on pre-therapeutic presumably healthy brain tissue. Assuming changes under therapy, the distinction between therapeutic effects and tumor progress is a challenging endeavor. This is further complicated by the fact that observed changes are also dependent on the therapeutic success [66].

31P-MRS, when interpreted along with other clinical and imaging parameters, constitutes an additional imaging biomarker for both outcome measurement or treatment response. This is of potential interest in radiomics studies, and could potentially enable a more reliable and reproducible non-invasive diagnosis and more individualized treatment planning.

At the moment this method is experimental and still has to be implemented in clinical investigation [33].

7. Conclusions

Proton MR-spectroscopy is a valuable addition to the conventional MR sequences in diagnosis, and especially in follow-up of patients with high-grade glioma. Furthermore, we believe that the spectroscopy techniques can be a valuable tool in research of glioma, and that the ^1H -, but also ^{31}P - and other types of spectroscopy can provide us with a new insight in the metabolism of a glioma tissue in vivo.

Author Contributions: Conceptualization, M.G., S.M., R.S. and A.E.G.; methodology, M.G., S.M., R.S. and A.E.G.; formal analysis, J.M., N.G., J.K., C.F.F. and T.J.; writing—original draft preparation, M.G.; writing—review and editing, all authors; visualization, M.G.; supervision, E.R.G. and A.E.G. All authors have read and agreed to the published version of the manuscript.

Funding: This research received no external funding.

Institutional Review Board Statement: Not applicable.

Informed Consent Statement: Not applicable.

Data Availability Statement: Not applicable.

Conflicts of Interest: The authors declare no conflict of interest.

Abbreviations

The following abbreviations are used in this manuscript:

KIAA1549	protein KIAA1549
BRAF	proto-oncogene B-Raf
NF1	NF1-Gene
ATRX	ATP-dependent helicase ATRX
CDKN2A/B	cyclin-dependent kinase inhibitor 2A
TSC2	tuberous sclerosis 2 gene
PRKCA	Protein Kinase C Alpha
MN1	meningioma (disrupted in balanced translocation) 1
MYB	MYB proto-oncogene
MYBL1	MYB proto-oncogene like 1 gene
FGFR	Fibroblast growth factor receptor
H3 K27	27th amino acid in Histone H3
TP53	transformation-related protein 53
ACVR1	Activin A receptor, type I
PDGFRA	platelet-derived growth factor receptor A
EGFR	epidermal growth factor receptor
EZH1	EZH inhibitory protein
IDH	Isocitrate dehydrogenase
MYCN	N-myc proto-oncogene protein
NTRK	neurotrophe tyrosin-receptor kinase
ALK	anaplastic lymphoma kinase
ROS	Reactive oxygen species
MET	mesenchymal-epithelial transition factor
TERT	telomerase reverse transcriptase
CIC	capicua
FUBP1	far upstream element binding protein 1
NOTCH1	Neurogenic locus notch homolog protein 1

References

1. Brennan, P.; Butler, H.; Christie, L.; Hegarty, M.; Jenkinson, M.; Keerie, C.; Norrie, J.; o'Brien, R.; Palmer, D.; Smith, B.; et al. Early diagnosis of brain tumours using a novel spectroscopic liquid biopsy. *Brain Commun.* **2021**, *3*, fcab056. [[CrossRef](#)] [[PubMed](#)]
2. Schneider, T.; Mawrin, C.; Scherlach, C.; Skalej, M.; Firsching, R. Gliomas in Adults. *Dtsch. Ärzteblatt Int.* **2010**, *107*, 799–807. [[CrossRef](#)] [[PubMed](#)]
3. Duc, N. The role of diffusion tensor imaging metrics in the discrimination between cerebellar medulloblastoma and brainstem glioma. *Pediatr. Blood Cancer* **2020**, *67*, e28468. [[CrossRef](#)] [[PubMed](#)]

4. Duc, N.M.; Huy, H.Q.; Nadarajan, C.; Keserci, B. The Role of Predictive Model Based on Quantitative Basic Magnetic Resonance Imaging in Differentiating Medulloblastoma from Ependymoma. *Anticancer Res.* **2020**, *40*, 2975–2980. [[CrossRef](#)] [[PubMed](#)]
5. Durmo, F.; Rydelius, A.; Baena, S.; Askaner, K.; Lätt, J.; Bengzon, J.; Englund, E.; Chenevert, T.; Björkman-Burtscher, I.; Maly Sundgren, P. Multivoxel H-MR Spectroscopy Biometrics for Preoperative Differentiation Between Brain Tumors. *Tomography* **2018**, *4*, 172–181. [[CrossRef](#)]
6. Weybright, P.; Maly Sundgren, P.; Maly, P.; Hassan, D.; Nan, B.; Rohrer, S.; Junck, L. Differentiation Between Brain Tumor Recurrence and Radiation Injury Using MR Spectroscopy. *AJR Am. J. Roentgenol.* **2005**, *185*, 1471–1476. [[CrossRef](#)]
7. Ellingson, B.; Bendszus, M.; Boxerman, J.; Barboriak, D.; Erickson, B.; Smits, M.; Nelson, S.; Gerstner, E.; Alexander, B.; Goldmacher, G.; et al. Consensus recommendations for a standardized Brain Tumor Imaging Protocol in clinical trials. *Neuro-Oncology* **2015**, *17*, 1188–1198. [[CrossRef](#)]
8. Malik, D.G.; Rath, T.J.; Urcuyo Acevedo, J.C.; Canoll, P.D.; Swanson, K.R.; Boxerman, J.L.; Quarles, C.C.; Schmainda, K.M.; Burns, T.C.; Hu, L.S. Advanced MRI Protocols to Discriminate Glioma From Treatment Effects: State of the Art and Future Directions. *Front. Radiol.* **2022**, *2*, 809373. [[CrossRef](#)]
9. Louis, D.; Perry, A.; Reifenberger, G.; Deimling, A.; Figarella-Branger, D.; Cavenee, W.; Ohgaki, H.; Wiestler, O.; Kleihues, P.; Ellison, D. The 2016 World Health Organization Classification of Tumors of the Central Nervous System: A summary. *Acta Neuropathol.* **2016**, *131*, 803–820. [[CrossRef](#)]
10. Louis, D.; Perry, A.; Wesseling, P.; Brat, D.; Cree, I.; Figarella-Branger, D.; Hawkins, C.; Ng, H.; Pfister, S.; Reifenberger, G.; et al. The 2021 WHO Classification of Tumors of the Central Nervous System: A summary. *Neuro-Oncology* **2021**, *23*, 1231–1251. [[CrossRef](#)]
11. Collins, V.; Jones, D.; Giannini, C. Pilocytic astrocytoma: Pathology, molecular mechanisms and markers. *Acta Neuropathol.* **2015**, *129*, 775–788. [[CrossRef](#)] [[PubMed](#)]
12. Bender, K.; Perez, E.; Chirica, M.; Onken, J.; Kahn, J.; Brenner, W.; Ehret, F.; Euskirchen, P.; Koch, A.; Capper, D.; et al. High-grade astrocytoma with piloid features (HGAP): The Charité experience with a new central nervous system tumor entity. *J. Neuro-Oncol.* **2021**, *153*, 109–120. [[CrossRef](#)] [[PubMed](#)]
13. Shaikh, N.; Brahmabhatt, N.; Kruser, T.J.; Kam, K.; Appin, C.; Wadhvani, N.; Chandler, J.; Md, P.; Lukas, R. Pleomorphic xanthoastrocytoma: A brief review. *CNS Oncol.* **2019**, *8*, CNS39. [[CrossRef](#)]
14. Giannikou, K.; Zhu, Z.; Kim, J.; Winden, K.; Tyburczy, M.; Marron, D.; Parker, J.; Hebert, Z.; Bongaarts, A.; Taing, L.; et al. Subependymal giant cell astrocytomas are characterized by mTORC1 hyperactivation, a very low somatic mutation rate and a unique gene expression profile. *Mod. Pathol.* **2020**, *34*, 264–279. [[CrossRef](#)] [[PubMed](#)]
15. Goode, B.; Mondal, G.; Hyun, M.; Ruiz, D.; Lin, Y.H.; Ziffle, J.; Joseph, N.; Onodera, C.; Talevich, E.; Grenert, J.; et al. A recurrent kinase domain mutation in PRKCA defines chordoid glioma of the third ventricle. *Nat. Commun.* **2018**, *9*, 810. [[CrossRef](#)] [[PubMed](#)]
16. Sturm, D.; Orr, B.; Toprak, U.; Hovestadt, V.; Jones, D.; Capper, D.; Sill, M.; Buchhalter, I.; Northcott, P.; Leis, I.; et al. New Brain Tumor Entities Emerge from Molecular Classification of CNS-PNETs. *Cell* **2016**, *164*, 1060–1072. [[CrossRef](#)] [[PubMed](#)]
17. Ellison, D.; Hawkins, C.; Jones, D.; Onar-Thomas, A.; Pfister, S.; Reifenberger, G.; Louis, D. cIMPACT-NOW update 4: Diffuse gliomas characterized by MYB, MYBL1, or FGFR1 alterations or BRAFV600E mutation. *Acta Neuropathol.* **2019**, *137*, 683–687. [[CrossRef](#)]
18. Huse, J.; Snuderl, M.; Jones, D.; Brathwaite, C.; Altman, N.; Lavi, E.; Saffery, R.; Sexton-Oates, A.; Blümcke, I.; Capper, D.; et al. Polymorphous low-grade neuroepithelial tumor of the young (PLNTY): An epileptogenic neoplasm with oligodendroglioma-like components, aberrant CD34 expression, and genetic alterations involving the MAP kinase pathway. *Acta Neuropathol.* **2017**, *133*, 417–429. [[CrossRef](#)]
19. Qaddoumi, I.; Orisme, W.; Wen, J.; Santiago, T.; Gupta, K.; Dalton, J.; Tang, B.; Hauptfear, K.; Punchihewa, C.; Easton, J.; et al. Genetic alterations in uncommon low-grade neuroepithelial tumors: BRAF, FGFR1, and MYB mutations occur at high frequency and align with morphology. *Acta Neuropathol.* **2016**, *131*, 833–845. [[CrossRef](#)]
20. Buczkowicz, P.; Bartels, U.; Bouffet, E.; Becher, O.; Hawkins, C. Histopathological spectrum of paediatric diffuse intrinsic pontine glioma: Diagnostic and therapeutic implications. *Acta Neuropathol.* **2014**, *128*, 573–581. [[CrossRef](#)]
21. Gianno, F.; Antonelli, M.; Dio, T.; Minasi, S.; Donofrio, V.; Buccoliero, A.; Gardiman, M.; Pollo, B.; Camassei, F.; Rossi, S.; et al. Correlation Between Immunohistochemistry and Sequencing in H3G34-Mutant Gliomas. *Am. J. Surg. Pathol.* **2021**, *45*, 200–204. [[CrossRef](#)] [[PubMed](#)]
22. Gessi, M.; Gielen, G.; Hammes, J.; Dörner, E.; Mühlen, A.; Waha, A.; Pietsch, T. H3.3 G34R mutations in pediatric primitive neuroectodermal tumors of central nervous system (CNS-PNET) and pediatric glioblastomas: Possible diagnostic and therapeutic implications? *J. Neuro-Oncol.* **2013**, *112*, 67–72. [[CrossRef](#)] [[PubMed](#)]
23. Schwartzentruber, J.; Korshunov, A.; Liu, X.; Jones, D.; Pfaff, E.; Jacob, K.; Sturm, D.; Fontebasso, A.; Khuong Quang, D.A.; Tönjes, M.; et al. Driver mutations in histone H3.3 and chromatin remodeling genes in pediatric glioblastoma. *Nature* **2012**, *482*, 226–231. [[CrossRef](#)] [[PubMed](#)]
24. Korshunov, A.; Schrimpf, D.; Ryzhova, M.; Sturm, D.; Chavez, L.; Hovestadt, V.; Sharma, T.; Habel, A.; Burford, A.; Jones, C.; et al. H3-/IDH-wild type pediatric glioblastoma is comprised of molecularly and prognostically distinct subtypes with associated oncogenic drivers. *Acta Neuropathol.* **2017**, *134*, 507–516. [[CrossRef](#)]

25. Guerreiro Stucklin, A.; Ryall, S.; Fukuoka, K.; Zápotocký, M.; Lassaletta, A.; Li, C.; Bridge, T.; Kim, B.; Arnoldo, A.; Kowalski, P.; et al. Alterations in ALK/ROS1/NTRK/MET drive a group of infantile hemispheric gliomas. *Nat. Commun.* **2019**, *10*, 4343. [[CrossRef](#)]
26. Yan, H.; Parsons, D.; Jin, G.; McLendon, R.; Rasheed, B.; Yuan, W.; Kos, I.; Batinic-Haberle, I.; Jones, S.; Riggins, G.; et al. IDH1 and IDH2 mutations in gliomas. *N. Engl. J. Med.* **2009**, *360*, 765–773. [[CrossRef](#)] [[PubMed](#)]
27. Nandakumar, P.; Mansouri, A.; Das, S. The role of ATRX in glioma biology. *Front. Oncol.* **2017**, *7*, 236. [[CrossRef](#)]
28. Capper, D.; Zentgraf, H.; Balss, J.; Hartmann, C.; Deimling, A. Monoclonal antibody specific for IDH1 R132H mutation. *Acta Neuropathol.* **2009**, *118*, 599–601. [[CrossRef](#)]
29. Liu, X.; Gerges, N.; Korshunov, A.; Sabha, N.; Khuong Quang, D.A.; Fontebasso, A.; Fleming, A.; Hadjadj, D.; Schwartzenruber, J.; Majewski, J.; et al. Frequent ATRX mutations and loss of expression in adult diffuse astrocytic tumors carrying IDH1/IDH2 and TP53 mutations. *Acta Neuropathol.* **2012**, *124*, 615–625. [[CrossRef](#)]
30. Pekmezci, M.; Rice, T.; Molinaro, A.; Hansen, H.; McCoy, L.; Tihan, T.; Giannini, C.; Eckel-Passow, J.; Lachance, D.; Wiencke, J.; et al. OS07.8 Adult infiltrating gliomas with WHO 2016 integrated diagnosis: Additional prognostic roles of ATRX and TERT. *Neuro-Oncology* **2017**, *19*, iii15. [[CrossRef](#)]
31. Siemens. *Syngo MR B19, Basic Manual-Spectroscopy*; Booklet; Siemens Healthineers AG: Munich, Germany, 2012.
32. Pinggera, D.; Steiger, R.; Bauer, M.; Kerschbaumer, J.; Luger, M.; Beer, R.; Rietzler, A.; Grams, A.; Gizewski, E.; Thomé, C.; et al. Cerebral Energy Status and Altered Metabolism in Early Severe TBI: First Results of a Prospective 31P-MRS Feasibility Study. *Neurocrit. Care* **2020**, *34*, 432–440. [[CrossRef](#)] [[PubMed](#)]
33. Rietzler, A.; Steiger, R.; Mangesius, S.; Walchhofer, L.M.; Gothe, R.M.; Schocke, M.; Gizewski, E.R.; Grams, A.E. Energy metabolism measured by 31P magnetic resonance spectroscopy in the healthy human brain. *J. Neuroradiol.* **2021**, *in press*. [[CrossRef](#)] [[PubMed](#)]
34. Hattingen, E.; Lanfermann, H.; Menon, S.; Neumann-Haefelin, T.; DuMesnil de Rochement, R.; Stamelou, M.; Höglinger, G.; Magerkurth, J.; Pilatus, U. Combined 1H and 31P MR spectroscopic imaging: Impaired energy metabolism in severe carotid stenosis and changes upon treatment. *Magn. Reson. Mater. Phys. Biol. Med.* **2009**, *22*, 43–52. [[CrossRef](#)] [[PubMed](#)]
35. Ostrom, Q.T.; Cioffi, G.; Waite, K.; Kruchko, C.; Barnholtz-Sloan, J.S. CBTRUS Statistical Report: Primary Brain and Other Central Nervous System Tumors Diagnosed in the United States in 2014–2018. *Neuro-Oncology* **2021**, *23*, iii1–iii105. [[CrossRef](#)] [[PubMed](#)]
36. Alrayahi, J.; Zápotocký, M.; Ramaswamy, V.; Hanagandi, P.; Branson, H.; Mubarak, W.; Raybaud, C.; Laughlin, S. Pediatric Brain Tumor Genetics: What Radiologists Need to Know. *RadioGraphics* **2018**, *38*, 7. [[CrossRef](#)]
37. Donia, M.; Abougabal, A.; Zakaria, Y.; Farhoud, A. Role of proton magnetic resonance spectroscopy in diagnosis of pilocytic astrocytoma in children. *Alex. J. Med.* **2012**, *48*, 131–137. [[CrossRef](#)]
38. Porto, L.; Kieslich, M.; Franz, K.; Lehrnbecher, T.; Zanella, F.; Pilatus, U.; Hattingen, E. MR spectroscopy differentiation between high and low grade astrocytomas: A comparison between paediatric and adult tumours. *Eur. J. Paediatr. Neurol. EJPN Off. J. Eur. Paediatr. Neurol. Soc.* **2010**, *15*, 214–221. [[CrossRef](#)]
39. Hasan, A.M.; Hasan, A.; Megally, H.; Khallaf, M.; Haseib, A. The combined role of MR spectroscopy and perfusion imaging in preoperative differentiation between high- and low-grade gliomas. *Egypt. J. Radiol. Nucl. Med.* **2019**, *50*, 72. [[CrossRef](#)]
40. Shakir, T.; Fengli, L.; Chenguang, G.; Chen, N.; Zhang, M.; Shaohui, M. 1H-MR spectroscopy in grading of cerebral glioma: A new view point, MRS image quality assessment. *Acta Radiol. Open* **2022**, *11*, 205846012210770. [[CrossRef](#)]
41. Grossman, R.; Yousem, D. *Neuroradiology: The Requisites*; Requisites in Radiology; Mosby: St. Louis, MO, USA, 2003.
42. Toyooka, M.; Kimura, H.; Uematsu, H.; Kawamura, Y.; Takeuchi, H.; Itoh, H. Tissue characterization of glioma by proton magnetic resonance spectroscopy and perfusion-weighted magnetic resonance imaging: Glioma grading and histological correlation. *Clin. Imaging* **2008**, *32*, 251–258. [[CrossRef](#)]
43. Öz, G.; Alger, J.; Barker, P.; Bartha, R.; Bizzi, A.; Boesch, C.; Bolan, P.; Brindle, K.; Cudalbu, C.; Dincer, A.; et al. Clinical Proton MR Spectroscopy in Central Nervous System Disorders. *Radiology* **2014**, *270*, 658–679. [[CrossRef](#)] [[PubMed](#)]
44. Siu, A.; Wind, J.; Iorgulescu, J.; Chan, T.; Yamada, Y.; Sherman, J. Radiation necrosis following treatment of high grade glioma—A review of the literature and current understanding. *Acta Neurochir.* **2011**, *154*, 191–201; discussion 201. [[CrossRef](#)] [[PubMed](#)]
45. Ruben, J.; Dally, M.; Bailey, M.; Smith, R.; McLean, C.; Fedele, P. Cerebral radiation necrosis: Incidence, outcomes, and risk factors with emphasis on radiation parameters and chemotherapy. *Int. J. Radiat. Oncol. Biol. Phys.* **2006**, *65*, 499–508. [[CrossRef](#)] [[PubMed](#)]
46. Chamberlain, M.; Glantz, M.; Chalmers, L.; Horn, A.; Sloan, A. Chamberlain, M.C.; Glantz, M.J.; Chalmers, L.; Van Horn, A.; Sloan, A.E. Early necrosis following concurrent Temodar and radiotherapy in patients with glioblastoma. *J. Neuro-Oncol.* **2007**, *82*, 81–83. [[CrossRef](#)]
47. Easaw, J.; Mason, W.; Perry, J.; Laperriere, N.; Eisenstat, D.; Del Maestro, R.; Belanger, K.; Fulton, D.; Macdonald, D. Canadian Recommendations for the Treatment of Recurrent or Progressive Glioblastoma Multiforme. *Curr. Oncol. (Toronto Ont.)* **2011**, *18*, e126–e136. [[CrossRef](#)]
48. Hygino da Cruz, L.C.; Rodriguez, I.; Domingues, R.; Gasparetto, E.; Sorensen, A. Pseudoprogression and Pseudoresponse: Imaging Challenges in the Assessment of Posttreatment Glioma. *AJNR. Am. J. Neuroradiol.* **2011**, *32*, 1978–1985. [[CrossRef](#)]
49. Kazda, T.; Bulik, M.; Pospisil, P.; Smrcka, M.; Slampa, P.; Jancalek, R. Advanced MRI increases the diagnostic accuracy of recurrent glioblastoma: Single institution thresholds and validation of MR spectroscopy and diffusion weighted MR imaging. *NeuroImage Clin.* **2016**, *11*, 316–321. [[CrossRef](#)]

50. Smith, E.; Carlos, R.; Junck, L.; Tsien, C.; Elias, A.; Maly Sundgren, P. Developing a Clinical Decision Model: MR Spectroscopy to Differentiate Between Recurrent Tumor and Radiation Change in Patients with New Contrast-Enhancing Lesions. *AJR Am. J. Roentgenol.* **2009**, *192*, W45–W52. [[CrossRef](#)]
51. Elias, A.E.; Carlos, R.C.; Smith, E.A.; Frechtling, D.; George, B.; Maly, P.; Sundgren, P.C. MR Spectroscopy Using Normalized and Non-normalized Metabolite Ratios for Differentiating Recurrent Brain Tumor from Radiation Injury. *Acad. Radiol.* **2011**, *18*, 1101–1108. [[CrossRef](#)]
52. Bulik, M.; Kazda, T.; Slampa, P.; Jancalek, R. The Diagnostic Ability of Follow-Up Imaging Biomarkers after Treatment of Glioblastoma in the Temozolomide Era: Implications from Proton MR Spectroscopy and Apparent Diffusion Coefficient Mapping. *BioMed Res. Int.* **2015**, *2015*, 641023. [[CrossRef](#)]
53. Zeng, Q.S.; Li, C.F.; Liu, H.; Zhen, J.H.; Feng, D.C. Distinction Between Recurrent Glioma and Radiation Injury Using Magnetic Resonance Spectroscopy in Combination with Diffusion-Weighted Imaging. *Int. J. Radiat. Oncol. Biol. Phys.* **2007**, *68*, 151–158. [[CrossRef](#)] [[PubMed](#)]
54. Amin, A.; Moustafa, H.; Ahmed, E.; El-Toukhy, M. Glioma residual or recurrence versus radiation necrosis: Accuracy of pentavalent technetium-99m-dimercaptosuccinic acid [Tc-99m (V) DMSA] brain SPECT compared to proton magnetic resonance spectroscopy (1H-MRS): Initial results. *J. Neuro-Oncol.* **2011**, *106*, 579–587. [[CrossRef](#)] [[PubMed](#)]
55. Sawlani, V.; Taylor, R.; Rowley, K.; Redfern, R.; Martin, J.; Poptani, H. Magnetic Resonance Spectroscopy for Differentiating Pseudo-Progression from True Progression in GBM on Concurrent Chemoradiotherapy. *Neuroradiol. J.* **2012**, *25*, 575–586. [[CrossRef](#)] [[PubMed](#)]
56. Walecki, J.; Sokół, M.; Pieniżek, P.; Maciejewski, B.; Tarnawski, R.; Krupska, T.; Wydmański, J.; Brzeziński, J.; Grieb, P. Role of short TE 1H-MR spectroscopy in monitoring of post-operation irradiated patients. *Eur. J. Radiol.* **1999**, *30*, 154–161. [[CrossRef](#)]
57. Rock, J.; Hearshen, D.; Scarpace, L.; Croteau, D.; Gutierrez, J.; Fisher, J.; Rosenblum, M.; Mikkelsen, T. Correlations between Magnetic Resonance Spectroscopy and Image-guided Histopathology, with Special Attention to Radiation Necrosis. *Neurosurgery* **2002**, *51*, 912–919; discussion 919. [[CrossRef](#)]
58. Barajas, R.; Chang, J.; Segal, M.; Parsa, A.; Mcdermott, M.; Berger, M.; Cha, S. Differentiation of Recurrent Glioblastoma Multiforme from Radiation Necrosis after External Beam Radiation Therapy with Dynamic Susceptibility-weighted Contrast-enhanced Perfusion MR Imaging. *Radiology* **2009**, *253*, 486–496. [[CrossRef](#)]
59. Van Dijken, B.; Laar, P.; Holtman, G.; Hoorn, A. Diagnostic accuracy of magnetic resonance imaging techniques for treatment response evaluation in patients with high-grade glioma, a systematic review and meta-analysis. *Eur. Radiol.* **2017**, *27*, 4129–4144. [[CrossRef](#)]
60. Fèvre, C.; Constans, J.M.; Chambrelant, I.; Antoni, D.; Bund, C.; Leroy-Freschini, B.; Schott, R.; Cebula, H.; Noël, G. Pseudoprogression versus true progression in glioblastoma patients: A multiapproach literature review. Part 2—Radiological features and metric markers. *Crit. Rev. Oncol.* **2021**, *159*, 103230. [[CrossRef](#)]
61. Anbarloui, M.; Ghodsi, S.; Khoshnevisan, A.; Khadivi, M.; Abdollahzade, S.; Aoude, A.; Naderi, S.; Najafi, Z.; Faghih-Jouibari, M. Accuracy of magnetic resonance spectroscopy in distinction between radiation necrosis and recurrence of brain tumors. *Iran. J. Neurol.* **2015**, *14*, 29–34.
62. Galijašević, M.; Steiger, R.; Radović, I.; Birkel-Toeglhofer, A.M.; Birkel, C.; Deeg, L.; Mangesius, S.; Rietzler, A.; Regodić, M.; Stockhammer, G.; et al. Phosphorus Magnetic Resonance Spectroscopy and Molecular Markers in IDH1 Wild Type Glioblastoma. *Cancers* **2021**, *13*, 3569. [[CrossRef](#)]
63. Wenger, K.; Steinbach, J.; Bähr, O.; Pilatus, U.; Hattingen, E. Lower Lactate Levels and Lower Intracellular pH in Patients with IDH-Mutant versus Wild-Type Gliomas. *Am. J. Neuroradiol.* **2020**, *41*, 1414–1422. [[CrossRef](#)] [[PubMed](#)]
64. Wenger, K.; Hattingen, E.; Franz, K.; Steinbach, J.; Bähr, O.; Pilatus, U. In vivo Metabolic Profiles as Determined by 31P and short TE 1H MR-Spectroscopy. *Clin. Neuroradiol.* **2019**, *29*, 27–36. [[CrossRef](#)] [[PubMed](#)]
65. Wenger, K.; Hattingen, E.; Franz, K.; Steinbach, J.; Bähr, O.; Pilatus, U. Intracellular pH measured by 31 P-MR-spectroscopy might predict site of progression in recurrent glioblastoma under antiangiogenic therapy: Intracellular pH Measured by 31 P-MR-S. *J. Magn. Reson. Imaging* **2017**, *46*, 1200–1208. [[CrossRef](#)] [[PubMed](#)]
66. Grams, A.E.; Mangesius, S.; Steiger, R.; Radovic, I.; Rietzler, A.; Walchhofer, L.M.; Galijašević, M.; Mangesius, J.; Nowosielski, M.; Freyschlag, C.F.; et al. Changes in Brain Energy and Membrane Metabolism in Glioblastoma following Chemoradiation. *Curr. Oncol.* **2021**, *28*, 5041–5053. [[CrossRef](#)] [[PubMed](#)]
67. Walchhofer, L.M.; Steiger, R.; Rietzler, A.; Kerschbaumer, J.; Freyschlag, C.; Stockhammer, G.; Gizewski, E.; Grams, A. Phosphorus Magnetic Resonance Spectroscopy to Detect Regional Differences of Energy and Membrane Metabolism in Naïve Glioblastoma Multiforme. *Cancers* **2021**, *13*, 2598. [[CrossRef](#)]
68. Hnilicova, P.; Richterova, R.; Zelenak, K.; Kolarovszki, B.; Majercikova, Z.; Hatok, J. Noninvasive study of brain tumours metabolism using phosphorus-31 magnetic resonance spectroscopy. *Bratisl. Lek. Listy* **2020**, *121*, 488–492. [[CrossRef](#)]
69. Maintz, D.; Heindel, W.; Kugel, H.; Jaeger, R.; Lackner, K.J. Phosphorus-31 MR spectroscopy of normal adult human brain and brain tumours. *NMR Biomed.* **2002**, *15*, 18–27. [[CrossRef](#)]
70. Bulakbasi, N.; Kocaoglu, M.; Sanal, H.; Tayfun, C. Efficacy of in vivo 31Phosphorus Magnetic Resonance Spectroscopy in Differentiation and Staging of Adult Human Brain Tumors. *Neuroradiol. J.* **2007**, *20*, 646–655. [[CrossRef](#)]

71. Hattingen, E.; Jurcoane, A.; Bähr, O.; Rieger, J.; Magerkurth, J.; Anti, S.; Steinbach, J.; Pilatus, U. Bevacizumab impairs oxidative energy metabolism and shows antitumoral effects in recurrent glioblastomas: A 31P/1H MRSI and quantitative magnetic resonance imaging study. *Neuro-Oncology* **2011**, *13*, 1349–1363. [[CrossRef](#)]
72. Ha, D.H.; Choi, S.; Oh, J.; Yoon, S.K.; Kang, M.; Kim, K.U. Application of 31P MR Spectroscopy to the Brain Tumors. *Korean J. Radiol. Off. J. Korean Radiol. Soc.* **2013**, *14*, 477–486. [[CrossRef](#)]
73. Kamble, R.B.; Jayakumar Peruvumba, N.; Shivashankar, R. Energy status and metabolism in intracranial space occupying lesions: A prospective 31p spectroscopic study. *J. Clin. Diagn. Res. JCDR* **2014**, *8*, RC05. [[CrossRef](#)] [[PubMed](#)]
74. Verma, G.; Chawla, S.; Mohan, S.; Wang, S.; Nasrallah, M.; Sheriff, S.; Desai, A.; Brem, S.; O'Rourke, D.; Wolf, R.; et al. Three-dimensional echo planar spectroscopic imaging for differentiation of true progression from pseudoprogression in patients with glioblastoma. *NMR Biomed.* **2018**, *32*, e4042. [[CrossRef](#)] [[PubMed](#)]